



## ORIGINAL ARTICLE

# Structural characterization of chlorogenic acid-metal complexes derived from the aqueous extracts of medicinal plants and their DNA cleavage and antibacterial activities



Kangkang Zheng, Yafeng Liu, Liang Peng\*, Zhimin Li\*, Wenbin Xu

Engineering Center of Jiangxi University for Fine Chemicals, School of Pharmacy, Jiangxi Science and Technology Normal University, Nanchang 330013, PR China

Received 13 December 2022; accepted 19 March 2023

Available online 23 March 2023

## KEYWORDS

Medicinal plant;  
Chlorogenic acid;  
Metal complexing;  
DNA cleavage;  
Antibiotics

**Abstract** The discovery of organic components with pharmacological activities in medicinal plants is crucial for new drug development. We examined chlorogenic acid (CGA) using high-performance liquid chromatography to analyze the aqueous and methanolic extracts of medicinal plants dissolved in methanol or methanol containing 15% formic acid. We found that for the aqueous extract, the peak areas of various components dissolved in 15% formic acid methanol were significantly larger than those dissolved in methanol. For the differences in the methanolic extract, the peak areas of all chromatographic peaks were relatively small between the samples dissolved in the two solvents. Electrospray ionization time-of-flight mass spectrometry showed that CGA could react in hot water with the eight most common plant metal ions ( $\text{Ca}^{2+}$ ,  $\text{Cu}^{2+}$ ,  $\text{Fe}^{3+}$ ,  $\text{Mg}^{2+}$ ,  $\text{Mn}^{2+}$ ,  $\text{Ni}^{2+}$ ,  $\text{Sr}^{2+}$ , and  $\text{Zn}^{2+}$ ) to form complexes with different coordination forms. The bioactivity experiments showed that CGA-Cu complexes could cause DNA cleavage through oxidative damage. CGA-Ni, CGA-Mn, and CGA-Zn showed significantly stronger inhibition against *Staphylococcus aureus* than CGA and the corresponding metal ions. These results suggest that, during the decoction process of medicinal plants, CGA forms complexes with metal ions, which are likely to be one of the active ingredients in medicinal plants. Subsequently, further research is needed on the antibacterial mechanism of chlorogenic acid-metal complexes not mentioned in this article.

© 2023 The Author(s). Published by Elsevier B.V. on behalf of King Saud University. This is an open access article under the CC BY-NC-ND license (<http://creativecommons.org/licenses/by-nc-nd/4.0/>).

\* Corresponding authors at: Engineering Center of Jiangxi University for Fine Chemicals, School of Pharmacy, Jiangxi Science and Technology Normal University, No. 605, Fenglin Avenue, Nanchang 330013, PR China.

E-mail addresses: [pengliang8036@163.com](mailto:pengliang8036@163.com) (L. Peng), [Lzmin3026@163.com](mailto:Lzmin3026@163.com) (Z. Li).

Peer review under responsibility of King Saud University.



Production and hosting by Elsevier

## 1. Introduction

The discovery of bioactive lead compounds in plants and their subsequent structural modification is an effective strategy for the research and development of innovative drugs, such as paclitaxel and vincristine for treating cancer; artemether and artemotil for treating malaria, and galantamine for treating Alzheimer's disease. The organic components in medicinal plants, which contain functional groups such as phenolic hydroxyl, sulfhydryl, and amine groups, are likely to form complexes with metal ions during extraction in medicinal plants. For example, Ruzik and Kwiatkowski (2018) detected the formation of numerous zinc (Zn) complexes with organic components in goji berry extract. Wojcieszek and Ruzik (2016) and Wojcieszek et al. (2017) detected the formation of various copper (Cu) complexes with phenolic compounds in acai and bilberry extracts. Borowska et al. (2020) detected the formation of Zn and Cu complexes with polyphenolic ingredients in chokeberry extract. Furthermore, previous studies have also shown that complexation between organic components and metal ions may enhance pharmacological activity. For example, Rutin-Zn (Ikeda et al., 2015), emodin-manganese (Mn) (Yang et al., 2014) and emodin-Cu (Mandal et al., 2017) complexes all have anticancer activities obviously stronger than their corresponding ligands and metal ions. The Rutin-nickel (Ni) complex not only has stronger antioxidant activity than free Rutin but also produces DNA cleavage effects absent from Rutin or  $\text{Ni}^{2+}$  alone (Raza et al., 2017). Furthermore, quercetin-iron complexes showed more potent antioxidant, antibacterial, and anti-obesity activities than quercetin alone (Imessaoudene et al., 2016), whereas also producing DNA cleavage activity that was absent when quercetin or iron ions acted alone (Raza et al., 2016). These findings suggest that the metal complexes formed between the organic components and the metal ions of plants during the extraction process show good bioactivity and warrant further investigation.

Chlorogenic acid (CGA) is a widely distributed phenolic compound in plants, mainly in roots, stems, flowers, leaves, and fruits. Modern pharmacological studies have found that CGA has antibacterial, antiviral, anticancer, antioxidant activities (Cai et al., 2019a), and is a potential treatment for Parkinson's disease (Singh et al., 2018; Singh et al., 2020). The structure of CGA (Fig. S1) comprises O-diphenol hydroxyl and carboxyl groups, which have relatively large conjugated systems and can easily form complexes with metal ions. In this study, high-performance liquid chromatography (HPLC) was time for the first implemented to analyze the aqueous and methanolic extracts of medicinal plants dissolved in methanol and 15% formic acid (FA) + methanol to confirm the presence of CGA-metal complexes in the aqueous extracts of plants. Ultraviolet-visible spectrophotometry (UV-Vis) and electrospray ionization time-of-flight mass spectrometry (ESI-TOF MS) were used to derive the structural characterization of the products of the reactions between CGA and the eight most common metal ions in plants ( $\text{Ca}^{2+}$ ,  $\text{Cu}^{2+}$ ,  $\text{Fe}^{3+}$ ,  $\text{Mg}^{2+}$ ,  $\text{Mn}^{2+}$ ,  $\text{Ni}^{2+}$ ,  $\text{Sr}^{2+}$ , and  $\text{Zn}^{2+}$ ) in hot water. Finally, the DNA cleavage and anti-*Staphylococcus aureus* activities of the reaction products were investigated. The search for lead compounds from natural medicinal plants mainly focuses on the organic components. This study indicates that there are various metal complexes in the aqueous extracts of natural medicinal plants, which may have good biological activities. Thus, this study will help identify new pharmacodynamic components of natural medicinal plants.

## 2. Materials and methods

### 2.1. Materials and reagents

Jin Yin Hua (JYH), Yu. Xing Cao (YXC), Du Zhong (DZ), and Sang Ye (SY) were purchased from Kangmei Pharmaceutical Co., Ltd. (Guangdong, China). Chinese herbs were identified by the Department of Pharmaceutical Botany,

School of Pharmacy, Jiangxi Science and Technology Normal University (Nanchang, China). JYH was identified as dried buds or the first blooming flowers of *Lonicera japonica* (Caprifoliaceae). YXC was identified as the dried aerial part of *Houttuynia cordata* Thunb. (Saururaceae). DZ was identified as the dried bark of *Eucommia ulmoides* Oliver (Eucommiaceae). SY was identified as the dried leaf of *Morus alba* L. (Moraceae).

CGA (purity > 98%) was purchased from Chengdu Desite Biotechnology Co., Ltd. (Chengdu, China). Methanol (MS-grade) was purchased from Merck KGaA (Darmstadt, Germany). FA (LC grade) was purchased from Aladdin Co., Ltd. (Shanghai, China). Anhydrous calcium chloride, copper chloride dihydrate, ferric chloride hexahydrate, magnesium chloride hexahydrate, manganese chloride tetrahydrate, nickel dichloride hexahydrate, strontium chloride hexahydrate, and anhydrous zinc chloride were purchased from Xilong Chemical Co., Ltd. (Guangdong, China). The pBR322 DNA was purchased from Sangon Biotech (Shanghai, China). *S. aureus* ATCC 25923 was purchased from the Henan Engineering Research Center of Industrial Microbial Strains (He Nan, China).

### 2.2. Instruments and equipment

The following instruments and equipment were used in this study: UV-2550 UV-Vis (Shimadzu Corp., Kyoto, Japan); Agilent 1260 HPLC system (Agilent Technologies, Santa Clara, CA, USA); Xevo G2-XS ESI-TOF-MS (Waters Corp., Milford, MA, USA); XS203S electronic precision balance (Mettler Toledo GmbH, Columbus, OH, USA); Hei-VAP rotary evaporator (Heidolph Instruments, Schwabach, Germany); Agilent 7700 inductively coupled plasma mass spectrometer (ICP-MS); DF-101S heat-collecting, constant-temperature magnetic stirrer (Henan Gongyi Yuhua Instrument Co., Ltd., Henan, China) with heating (Henan Gongyi Yuhua Instrument Co., Ltd., Henan, China); Mini-PROTEAN4 electrophoresis system (with PowerPac Basic power supply) (Bio-Rad Laboratories, Hercules, CA, USA); JY04s-3c gel imaging analysis system (Beijing Junyi Electrophoresis Co., Ltd., Beijing, China); LDZH-50KBS vertical pressure steam sterilizer (Shanghai ShenAn Medical Instrument Factory, Shanghai, China); and SPX-150 biochemical incubator (Shanghai Ke Heng Industrial Co., Ltd., Shanghai, China).

### 2.3. Confirming the presence of CGA-metal complexes in plant extracts

Four kinds of medicinal plants with high CGA content were selected: JYH, YXH, DZ, and SY. They were crushed and passed through a 20-mesh sieve, dried in an oven at 50 °C to a constant weight, and distilled water was added in a solid-to-liquid ratio of 1:20. The mixture was then soaked at 25 °C for 30 min, refluxed at 100 °C for 3 h, and filtered under reduced pressure. The filtrate was accurately divided into two aliquots and concentrated to dryness under reduced pressure to obtain the aqueous extract. The aqueous extract was then dissolved in an equal volume of methanol or 15% FA-methanol, ultrasonicated for 2 min, filtered with a 0.22 µm filter membrane, and subjected to HPLC.

The same methods were applied to prepare the methanol extracts of the four medicinal plants, which were then dissolved in methanol or 15% FA-methanol (extraction temperature: 70 °C) and subjected to HPLC.

The HPLC conditions were as follows: chromatography column, Agilent Eclipse XDB-C18 (4.6 × 250 mm, 5 μm); detection wavelength, 327 nm; column temperature, 30 °C; flow rate, 1.0 mL/min; injection volume, 10 μL; mobile phase A for 0.1% FA-H<sub>2</sub>O and C for methanol. The gradient elution conditions for the JYH, DZ, and SY samples were as follows: 0–90 min, 10% C → 100% C; 90–100 min, 100% C. The gradient elution conditions for the YXC samples were as follows: 0–5 min, 20% C; 5–10 min, 20–30% C; 10–15 min, 30% C; 15–70 min, 30% B–100% C; 70–80 min, 100% C.

$$\text{Peak area increase} = \frac{PA_{FM} - PA_M}{PA_M} \times 100\% \quad (1)$$

Where  $PA_{FM}$  is the peak area of samples dissolved in 15% FA-methanol, and  $PA_M$  is the peak area of samples dissolved in methanol.

#### 2.4. Measurement of the metal-ion content in the aqueous extracts of the four medicinal plants

The aqueous extracts of the four medicinal plants were prepared according to the methods described in Section 3.1. After drying in an oven at 50 °C to a constant weight, 100.00 mg of the samples were accurately weighed, dissolved in methanol or 15% FA-methanol using an ultrasonicator, centrifuged at 5,000 × *g*, and concentrated until dryness under reduced pressure. The dried samples were transferred to the container using 8 mL of aqua regia, to which 2 mL of hydrogen peroxide was added. Subsequently, they were well mixed and heated at 150 °C for 40 min. Subsequently, the samples were cooled to 25 °C and filtered, and the filtrate was diluted with ultrapure water to 50 mL for ICP-MS detection.

ICP-MS was performed under the following conditions: radio frequency power, 1.5 kW; plasma gas flow rate, 15.0 L/min; auxiliary gas flow rate, 1.00 L/min; and atomizer flow rate, 0.10 L/min.

### 2.5. Structural characterization of CGA-metal complexes

#### 2.5.1. UV-vis detection

UV-vis absorption spectra of chlorogenic acid and chlorogenic acid-metal complexes were determined by a UV-Vis spectrophotometer (Cai et al., 2019b). CGA (0.02 mmol) was accurately weighed and placed with 0.01 mmol of anhydrous calcium chloride, magnesium chloride hexahydrate, anhydrous zinc chloride, ferric chloride hexahydrate, copper chloride dihydrate, nickel dichloride hexahydrate, manganese chloride tetrahydrate, or strontium chloride hexahydrate in a round-bottom flask. Then, 20 mL of distilled water was added and mixed well, which reacted at 100 °C while heating under reflux and magnetic stirring for 3 h. Two aliquots (2 mL each) were obtained from the reaction solution, while hot and diluted 10 times with distilled water and 15% FA-H<sub>2</sub>O solution preheated to 75 °C. After mixing, the solution was centrifuged at 6,000 × *g* for 8 min, and the supernatant was obtained, the UV-Vis spectrum was measured at the wavelength range

of 240 to 700 nm. The same methods were used to measure the UV-Vis absorption spectrum of CGA.

#### 2.5.2. ESI-TOF MS analysis of CGA-metal complexes

The reaction solution (2 mL) was centrifuged at 6,000 × *g* for 8 min and the resulting supernatant was subjected to ESI-TOF MS analysis. ESI was performed in the sample injection positive-ion mode, the sample injection infusion method was adopted for MS, the injection flow rate was 10 μL/min, and the mass detection range was 100–1,500. The drying gas flow rate was 800 L/h, and the temperature was 500 °C (Cai et al., 2019b).

#### 2.5.3. Identification of ferrous ions

Distilled water (20 mL) was added to 0.02 mol of CGA, 0.01 mol of FeCl<sub>3</sub>, 0.01 mol of FeCl<sub>2</sub>, and the mixture of 0.02 mol of CGA and 0.01 mol of FeCl<sub>3</sub> and reacted under the conditions described in Section 3.3.1. Then, 2 mL of the reaction solution was centrifuged at 6,000 × *g* for 8 min, followed by the addition of 1 mL of 1,10-phenanthroline solution with a mass fraction of 0.1% (first dissolved with a little ethanol, and then diluted with distilled water) and 1 mL acetic acid-sodium acetate buffer solution (pH 4.5) to the supernatant. After well mixing, the solution was left to stand for 150 s and color changes were observed.

### 2.6. DNA cleavage activity of CGA-metal complexes

#### 2.6.1. DNA cleavage activity

Reactions were performed according to the conditions described previously (Wang J. et al., 2010). The reaction solution was concentrated to dryness under reduced pressure and dissolved in dimethyl sulfoxide (DMSO) to prepare a 4 mmol/L solution (calculated based on the molar mass of CGA) for later use. In addition, equal amounts of CGA and eight types of metal salts were obtained to prepare solutions of equal concentrations using DMSO.

Eight microliters of distilled water, 10 μL of Buffer 1, 1 μL of sample solution, and 1 μL of pBR322 DNA were well mixed and allowed to react at 37 °C for 24 h. Once the reaction was complete, 4 μL of Buffer 2 was added, mixed well, and 5 μL of the resulting solution was loaded into the wells of agarose gel (0.32 g agarose, 40 mL Buffer 3) for electrophoresis at 120 mV for 1 h. The gel was then stained with 0.5 mg/L of Gel Red solution for 2 h, and the results were observed and recorded using a gel imager.

#### 2.6.2. Mechanism of DNA cleavage by CGA-Cu complexes

Ten microliters of Buffer 1, 1 μL of CGA and Cu<sup>2+</sup> reaction products in DMSO solution (CGA final concentration: 100 μmol/L, Cu<sup>2+</sup> final concentration: 50 μmol/L), 1 μL pBR322 DNA, and 8 μL of distilled water were mixed, followed by the addition of NaN<sub>3</sub> (final concentration: 100 mmol/L), EDTA (final concentration: 5 mmol/L), TEMPO (final concentration: 10 mmol/L), mannitol (final concentration: 100 mmol/L), catalase (CAT, final concentration: 4 U/μL), or superoxide dismutase (SOD, final concentration: 4 U/μL). After well mixing well and reacting at 37 °C for 1 h, 4 μL of Buffer 2 was added, and gel electrophoresis was performed according to the methods described in Section 3.4.1.

- Buffer 1: 10 mmol/L  $\text{KH}_2\text{PO}_4$ , 10 mmol/L NaCl, pH 7.2
- Buffer 2: 0.05% bromophenol blue, 36% glycerol, and 30 mmol/L of  $\text{Na}_2\text{H}_2\text{EDTA}$
- Buffer 3: 89 mmol/L tris–borate, 2 mmol/L  $\text{Na}_2\text{H}_2\text{EDTA}$

### 2.7. Antibacterial activity of CGA-metal complexes

Reactions were performed using 0.12 mmol of CGA and 0.06 mmol each of the eight metal salts according to the reaction conditions described previously. Briefly, the reaction solution was concentrated to dryness under reduced pressure, and distilled water containing 20% DMSO (V/V) was used to prepare a 24 mmol/L drug solution (calculated based on the molar mass of CGA) for later use.

*Staphylococcus aureus* was inoculated into fresh tryptic soy broth (TSB), incubated at 37 °C and 220 rpm for 12 h, and then transferred to fresh TSB at an inoculum size of 0.1% volume fraction for later use.

A set of seven sterilized test tubes was prepared for each group, 1 mL of drug solution was added to the first test tube, 500  $\mu\text{L}$  of distilled water was added to the 2nd–7th test tubes, and the 7th test tube was used as the blank control. Then 500  $\mu\text{L}$  of drug solution was obtained from the first test tube, added to the second test tube, and mixed well. Two-fold serial dilutions were performed in this manner until the sixth test tube, from which 500  $\mu\text{L}$  of solution was obtained and discarded. A bacterial solution (2 mL) was added to each of the seventh test tubes, then incubated at 37 °C for 18 h. Next, 10  $\mu\text{L}$  of the solution was obtained in the test tube, smeared

on prepared solid medium, and incubated at 37 °C for another 18 h, and the results were recorded.

## 3. Results

### 3.1. Confirming the presence of CGA-metal complexes in plant extracts

#### 3.1.1. Investigation on linear relationships and precision

Methanol was used to prepare a 3.2 mmol/L CGA stock solution and diluted twice to arrive at sample concentrations of 1.6, 0.8, 0.4, 0.2, 0.1, 0.05, 0.025, and 0.0125 mmol/L. Quantitative measurement of the CGA peak area was performed based on the HPLC conditions described in Section 2.3. Using the CGA peak area as the  $y$ -axis and the sample concentration as the  $x$ -axis, we obtained the regression equation for CGA:  $y = 8.559x - 121.39$  ( $R^2 = 0.9993$ ). This implies that CGA shows a good linear relationship within the range of 0.0125–3.2 mmol/L.

Chlorogenic acid control solutions of 0.0125, 0.8, and 3.2 mmol/L were injected six times and analyzed according to HPLC conditions in Section 3.1. The relative standard deviation of the peak area was less than 2%, suggesting that the instrument had good precision for high-, medium-, and low-concentration samples.

#### 3.1.2. Effect of different extraction solvents on the formation of CGA-metal complexes

CGA dissolved in methanol showed maximum absorbance at 243, 296, and 327 nm. To reduce the interference of impurities,

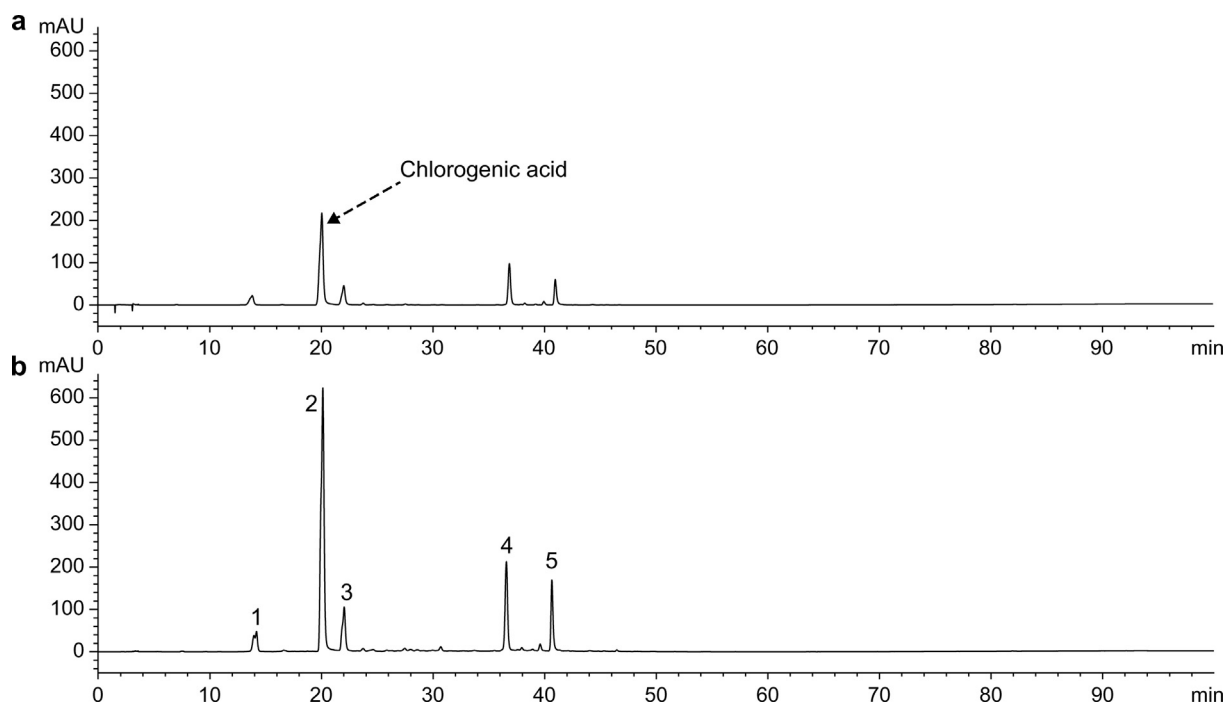


**Fig. 1** HPLC spectra of aqueous extracts of JYH dissolved in two solvents (327 nm). (a) Samples dissolved in methanol. (b) Samples dissolved in FA-methanol.

327 nm was selected as the detection wavelength for HPLC. The HPLC chromatograms of aqueous and methanolic extracts of JYH dissolved in equal volumes of 15% FA-methanol and methanol are shown in Figs. 1 and 2, whereas the detection results are shown in Tables 1. The peak area increase of CGA in the plant extract samples dissolved in two solvents is shown in Fig. 3.

As shown in Figs. 1 and 2, the number and retention time of the chromatographic peaks were essentially the same for aqueous and methanolic extracts of JYH dissolved in methanol and 15% FA-methanol. This indicates that adding an appropriate amount of FA to methanol did not lead to changes in the types of chemical compounds. Based on the data in Table 1, the samples of aqueous extracts dissolved in

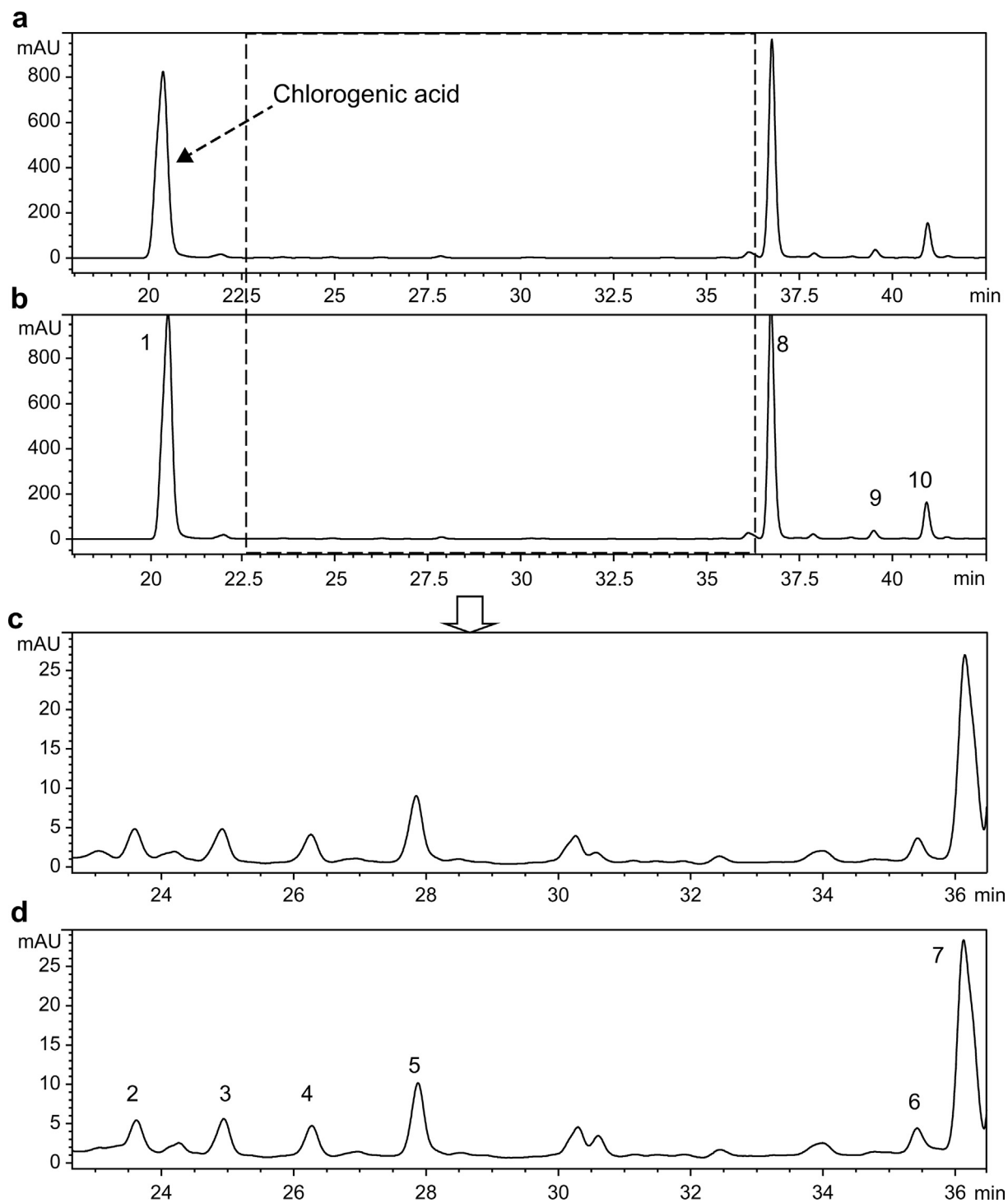


**Fig. 2** HPLC spectra of methanol extracts of JYH dissolved in two solvents (327 nm). (a) Samples dissolved in methanol. (b) Samples dissolved in FA-methanol.

15% FA-methanol showed significantly higher peak areas for various compounds, including CGA, and the peak area for CGA increased by 158.4%. In contrast, the methanolic extract samples dissolved in the two solvents showed increases in the peak area of less than 10%, of which the peak area of CGA in samples dissolved with 15% FA-methanol increased by only 3.62%. The HPLC results of extracts from the other three medicinal plants were like those of JYH (HPLC spectra and results for the other three extracts are shown in Figs. S2–S7 and Tables S1–S3).

### 3.2. Measurement of metal-ion content in the aqueous extracts of the four medicinal plants

Previous studies have found that samples of aqueous plant extracts dissolved in 15% FA-methanol showed varying degrees of increase in the peak areas of the organic compo-

nents compared to samples dissolved in methanol. Therefore, ICP-MS was performed to determine the contents of eight metal ions ( $\text{Ca}^{2+}$ ,  $\text{Cu}^{2+}$ ,  $\text{Fe}^{3+}$ ,  $\text{Mg}^{2+}$ ,  $\text{Mn}^{2+}$ ,  $\text{Ni}^{2+}$ ,  $\text{Sr}^{2+}$  and  $\text{Zn}^{2+}$ ) in the two types of samples. As shown in Fig. 4, the contents of the eight metal elements in the aqueous extract of JYH dissolved in 15% FA-methanol increased to different degrees compared to samples dissolved in methanol. This suggests that the addition of an appropriate amount of FA to methanol can promote the decomposition of some metal complexes that are insoluble in methanol, increasing the content of metal elements. Furthermore, among the eight metal elements, Mn showed the largest increase (1,300%), whereas Zn showed the smallest increase (12.31%), reflecting the varied abilities of different metals to form complexes with organic components or substantial differences in the stabilities of the metal complexes (the contents of the eight metal ions in four aqueous extracts dissolved in different solvents are shown in Table S4).

**Table 1** HPLC results of aqueous and methanol extracts of JYH dissolved in two solvents (n = 3).

Sample	Peak no.	Methanol		FA-methanol		Increase in peak area (%)
		Retention time (min)	Peak area	Retention time (min)	Peak area	
aqueous extracts	1	13.8 ± 0.39	550.8 ± 38.56	14.17 ± 0.99	599.4 ± 38.36	8.82
	2	20.04 ± 0.46 (CGA)	4,687.7 ± 285.95	20.11 ± 1.39	12,116.7 ± 654.3	158.48
	3	22.01 ± 0.22	904.2 ± 57.87	22.03 ± 1.41	1964.9 ± 117.89	117.31
	4	36.64 ± 0.81	1,508.4 ± 104.08	36.56 ± 2.52	3,307.5 ± 198.45	119.27
	5	40.96 ± 0.9	825.4 ± 46.22	40.64 ± 2.56	2,136.4 ± 134.59	158.83
methanol extracts	1	20.38 ± 1.3 (CGA)	17,954.7 ± 1,167.06	20.52 ± 1.4	18,604.2 ± 948.81	3.62
	2	23.60 ± 0.82	51.45 ± 14.86	23.62 ± 1.32	58.47 ± 15.24	13.64
	3	24.92 ± 1.29	68.95 ± 37.29	24.94 ± 1.88	69.84 ± 29.82	1.29
	4	26.26 ± 1.56	54.40 ± 12.47	26.28 ± 0.94	56.90 ± 9.64	4.60
	5	27.85 ± 2.47	127.61 ± 23.85	27.88 ± 1.99	132.68 ± 19.75	3.97
	6	36.15 ± 1.99	432.58 ± 23.79	36.13 ± 1.81	442.02 ± 28.73	2.18
	7	36.76 ± 2.35	12,583.2 ± 805.32	36.74 ± 1.98	12,982.5 ± 714.04	3.17
	8	37.9 ± 2.39	270.46 ± 13.52	37.87 ± 2.65	276.47 ± 18.8	2.22
	9	39.54 ± 2.14	459.46 ± 29.86	39.5 ± 2.61	455.41 ± 30.51	-0.88
	10	40.95 ± 2.33	2,020.61 ± 105.07	40.92 ± 2.5	2,075.59 ± 105.86	2.72

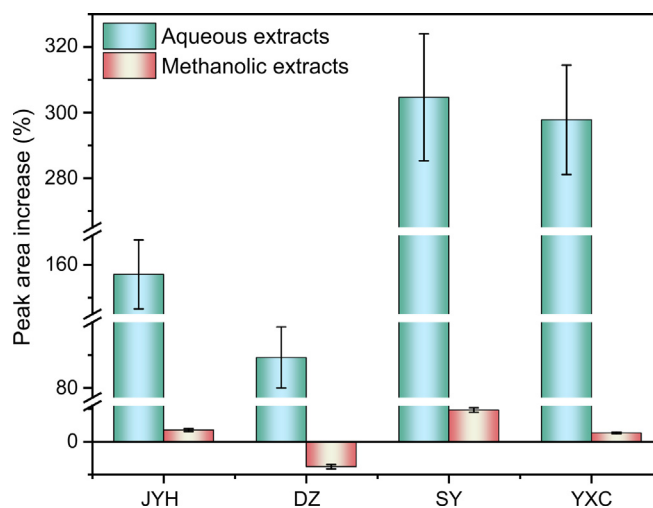


**Fig. 3** Peak area increase (%) of CGA in the four plant extracts dissolved in two solvents (n = 3).

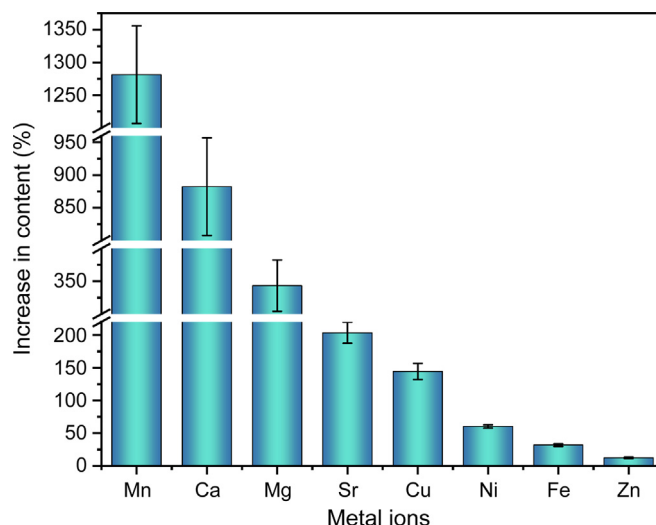


**Fig. 4** Content increase (%) of the eight metal ions in JYH aqueous extract dissolved in two solvents ( $n = 3$ ).

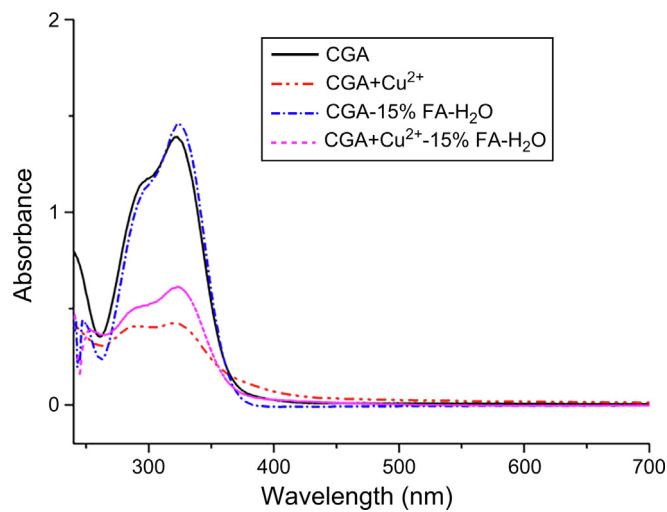


**Fig. 5** UV-Vis absorption spectra of CGA and CGA-Cu complexes in different solvents.

### 3.3. Structural characterization of CGA-metal complexes

#### 3.3.1. UV-vis analysis

The UV-Vis absorption spectra of the CGA and CGA-Cu complexes dissolved in water and 15% FA-H<sub>2</sub>O are shown in Fig. 5. The figure shows that the absorption spectra of CGA were essentially consistent between water and 15% FA-H<sub>2</sub>O. The maximum absorption wavelength was 327 nm, and the absorbance increased from 1.39 (water) to 1.46 (15% FA-H<sub>2</sub>O), which suggests that adding an appropriate amount of FA did not affect the UV-Vis spectra of CGA. The UV-Vis absorption spectrum of the CGA and Cu<sup>2+</sup> reaction supernatant showed notable changes compared to that of the CGA. Although the maximum absorption wavelength remained at 327 nm, the absorbance at this wavelength decreased by 69.09%, which implies that new products were formed by the reaction between CGA and Cu<sup>2+</sup> in hot water.

Furthermore, the addition of FA to the reaction solution caused the absorbance at 327 nm to increase from 0.43 to 0.61, which may be because of the decomposition of some CGA-Cu complexes into CGA and Cu<sup>2+</sup> in the FA-H<sub>2</sub>O solution. The UV-Vis absorption spectra of the CGA and Fe<sup>3+</sup> reaction supernatants (Fig. S8-d) showed changes similar to those presented in Fig. 5. After CGA reacted with the other six metal ions (Fig. S8), the maximum absorption wavelength was also at 327 nm; however, the absorbance at this wavelength increased to varying degrees compared to that of CGA. Adding an appropriate amount of FA led to different changes in absorbance. Specifically, the absorbance of the reaction supernatant for CGA with Ca<sup>2+</sup>, Mg<sup>2+</sup>, and Ni<sup>2+</sup> decreased to different extents, that with Zn<sup>2+</sup> basically remained unchanged, and that with Mn<sup>2+</sup> and Sr<sup>2+</sup> increased to different extents. Thus, CGA can form complexes with all eight metal ions in hot water, and these complexes can be partially decomposed in an acidic solution.

### 3.3.2. ESI-TOF MS analysis of CGA-metal complexes

The ESI-TOF MS results of the supernatant from the reaction of CGA with the eight metal ions in hot water are shown in Table 2. The table shows that the eight metal ions selected for this study formed complexes with CGA in hot water in various ratios. Using the reaction products of CGA and  $\text{Mn}^{2+}$  as an example, in the positive-ion mode of ESI, unreacted CGA ( $m/z = 355.1031$ ) and compounds with  $m/z$  of 408.0253, 762.1203, 815.0424, 1,116.2197, and 1,169.1381 were detected in the reaction supernatant. Based on the comparisons of accurate molecular weights and isotopic distributions (Fig. 6-1-5), we speculated that these five compounds were quasi-molecular ions of  $\text{M}^+$  or  $[\text{M}^+\text{H}]^+$  complexes formed by CGA and  $\text{Mn}^{2+}$  at ratios of 1:1, 2:1, 2:2, 3:1, and 3:2.

Besides  $\text{Fe}^{3+}$ , CGA formed complexes with the other six metal ions similar to those formed with  $\text{Mn}^{2+}$ . CGA formed complexes with  $\text{Ni}^{2+}$  at ratios of 1:1, 2:1, 2:2, and 3:2, with  $\text{Sr}^{2+}$  at ratios of 1:1, 2:1, 2:2, and 3:1; with  $\text{Ca}^{2+}$  at ratios of 2:1, 3:1, and 3:2, with  $\text{Mg}^{2+}$  at ratios of 3:1 and 3:2; with  $\text{Zn}^{2+}$  at ratios of 1:1 and 2:1; and with  $\text{Cu}^{2+}$  at ratios of 1:1, 2:1, and 2:2.

In the CGA and  $\text{Fe}^{3+}$  reaction supernatant, CGA formed complexes with  $m/z = 408.0149$ , 409.0227, 762.1095, 763.1184, 1,116.2052, and 1,117.2120. Among them,  $m/z = 408.0149$  was close to the theoretical molecular weight of  $\text{C}_{16}\text{H}_{18}\text{O}_9\text{Fe}$ , and the theoretical isotopic distributions of the two were essentially consistent (Fig. 7a and c). Therefore, we speculated that this was a  $[\text{L} + \text{Fe}^{3+} - 2\text{H}]^+$  compound

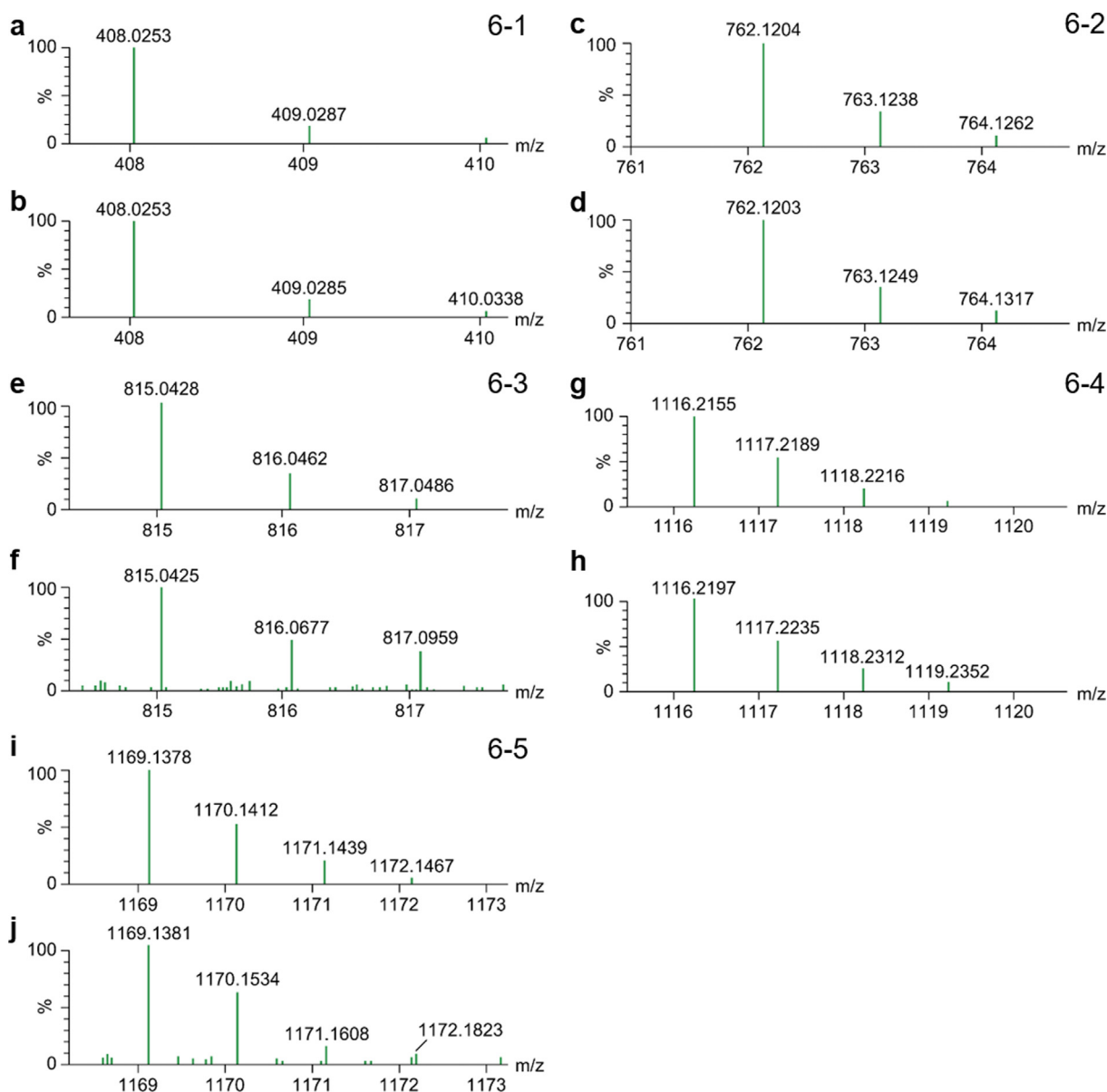


**Fig. 6** Theoretical (a) and measured (b) isotopic distributions of compound  $\text{C}_{16}\text{H}_{17}\text{O}_9\text{Mn}$ . Theoretical (c) and measured (d) isotopic distributions of compound  $\text{C}_{32}\text{H}_{35}\text{O}_{18}\text{Mn}$ . Theoretical (e) and measured (f) isotopic distributions of compound  $\text{C}_{32}\text{H}_{33}\text{O}_{18}\text{Mn}_2$ . Theoretical (g) and measured (h) isotopic distributions of compound  $\text{C}_{48}\text{H}_{53}\text{O}_{27}\text{Mn}$ . Theoretical (i) and measured (j) isotopic distributions of compound  $\text{C}_{48}\text{H}_{51}\text{O}_{27}\text{Mn}_2$ .

**Table 2** ESI-TOF-MS results for the reaction solutions of CGA and eight metal ions (ESI: positive-ion mode, L: CGA).

Source of reaction supernatant	$m/z$		Molecular formula	Possible structure	Comparison of the theoretical and measured isotopic distributions
	Theoretical value	Measured value			
All samples	355.1029	355.1031	$C_{16}H_{19}O_9$	$[L + H]^+$	
CGA and $Ca^{2+}$	747.1450	747.1452	$C_{32}H_{35}O_{18}Ca$	$[2L + Ca^{2+} - H]^+$	Fig. S9a, b
	1,101.2400	1,101.2443	$C_{48}H_{53}O_{27}Ca$	$[3L + Ca^{2+} - H]^+$	Fig. S9c, d
	1,139.1870	1,139.1869	$C_{48}H_{51}O_{27}Ca_2$	$[3L + 2Ca^{2+} - 3H]^+$	Fig. S9e, f
CGA and $Mg^{2+}$	1,085.2625	1,085.2649	$C_{48}H_{53}O_{27}Mg$	$[3L + Mg^{2+} - H]^+$	Fig. S10a, b
	1,107.2318	1,107.2305	$C_{48}H_{51}O_{27}Mg_2$	$[3L + 2Mg^{2+} - 3H]^+$	Fig. S10c, d
	CGA and $Zn^{2+}$	417.0164	417.0164	$C_{16}H_{17}O_9Zn$	$[L + Zn^{2+} - H]^+$
CGA and $Cu^{2+}$	771.1115	771.1116	$C_{32}H_{35}O_{18}Zn$	$[2L + Zn^{2+} - H]^+$	Fig. S11c, d
	416.0168	416.0168	$C_{16}H_{17}O_9Cu$	$[L + Cu^{2+} - H]^+$	Fig. S12a, b
	770.1119	770.1119	$C_{32}H_{35}O_{18}Cu$	$[2L + Cu^{2+} - H]^+$	Fig. S12c, d
CGA and $Ni^{2+}$	831.0259	831.0255	$C_{32}H_{33}O_{18}Cu_2$	$[2L + 2Cu^{2+} - 3H]^+$	Fig. S12e, f
	411.0226	411.0355	$C_{16}H_{17}O_9Ni$	$[L + Ni^{2+} - H]^+$	Fig. S13a, b
	765.1177	765.1177	$C_{32}H_{35}O_{18}Ni$	$[2L + Ni^{2+} - H]^+$	Fig. S13c, d
CGA and $Mn^{2+}$	821.0374	821.0380	$C_{32}H_{33}O_{18}Ni_2$	$[2L + 2Ni^{2+} - 3H]^+$	Fig. S13e, f
	1,175.1324	1,175.1332	$C_{48}H_{51}O_{27}Ni_2$	$[3L + 2Ni^{2+} - 3H]^+$	Fig. S13g, h
	408.0253	408.0253	$C_{16}H_{17}O_9Mn$	$[L + Mn^{2+} - H]^+$	Fig. 6a, b
CGA and $Sr^{2+}$	762.1204	762.1203	$C_{32}H_{35}O_{18}Mn$	$[2L + Mn^{2+} - H]^+$	Fig. 6c, d
	815.0428	815.0425	$C_{32}H_{33}O_{18}Mn_2$	$[2L + 2Mn^{2+} - 3H]^+$	Fig. 6e, f
	1,116.2155	1,116.2197	$C_{48}H_{53}O_{27}Mn$	$[3L + Mn^{2+} - H]^+$	Fig. 6g, h
CGA and $Fe^{3+}$	1,169.1378	1,169.1381	$C_{48}H_{51}O_{27}Mn_2$	$[3L + 2Mn^{2+} - 3H]^+$	Fig. 6i, j
	440.9930	440.9929	$C_{16}H_{17}O_9Sr$	$[L + Sr^{2+} - H]^+$	Fig. S14a, b
	795.0883	795.0883	$C_{32}H_{35}O_{18}Sr$	$[2L + Sr^{2+} - H]^+$	Fig. S14c, d
CGA and $Fe^{3+}$	880.9785	880.9789	$C_{32}H_{33}O_{18}Sr_2$	$[2L + 2Sr^{2+} - 3H]^+$	Fig. S14e, f
	1,149.1836	1,149.1864	$C_{48}H_{53}O_{27}Sr$	$[3L + Sr^{2+} - H]^+$	Fig. S14g, h
	408.0144	408.0147	$C_{16}H_{16}O_9Fe(III)$	$[L + Fe^{3+} - 2H]^+$	Fig. 7
CGA and $Fe^{3+}$	409.0222	409.0231	$C_{16}H_{17}O_9Fe(II)$	$[L + Fe^{2+} - H]^+$	
	762.1095	762.1100	$C_{32}H_{34}O_{18}Fe(III)$	$[2L + Fe^{3+} - 2H]^+$	
	763.1174	763.1174	$C_{32}H_{35}O_{18}Fe(II)$	$[2L + Fe^{2+} - H]^+$	
	1,116.2047	1,116.2051	$C_{48}H_{52}O_{27}Fe(III)$	$[3L + Fe^{3+} - 2H]^+$	
	1,117.2125	1,117.2130	$C_{48}H_{53}O_{27}Fe(II)$	$[3L + Fe^{2+} - H]^+$	

formed by CGA and  $Fe^{3+}$  in a 1:1 ratio. Because  $[L + Fe^{3+} - 2H]^+$  carries one positive charge, it was detected as  $M^+$  in the positive-ion mode of ESI. Furthermore, when analyzing the measured isotopic distribution,  $m/z = 409.0227$  was close to the theoretical molecular weight of  $C_{16}H_{18}O_9Fe(II)$ , and the isotopic distributions of the two were essentially consistent (Fig. 7b and c). CGA is an antioxidant, whereas  $Fe^{3+}$  has strong oxidizing properties. Therefore, by combining the properties of the two, we speculated that a portion of  $Fe^{3+}$  was reduced to  $Fe^{2+}$  during the reaction process and then formed complexes with CGA in a ratio of 1:1 to yield  $C_{16}H_{18}O_9Fe(II)$ . To determine whether  $Fe^{2+}$  was present in the reaction supernatant, 1,10-phenanthroline, which is a common reagent to identify  $Fe^{2+}$ , was used to perform chromogenic assays. The reaction results are shown in Fig. S16. The figure shows that no color changes were detected after the addition of 1,10-phenanthroline to the CGA and  $FeCl_3$  solutions, whereas a reddish-orange appearance was detected after 1,10-phenanthroline was added to the  $FeCl_2$  solution and the reaction supernatant for CGA and  $FeCl_3$ . This implies that  $Fe^{2+}$  was produced in the reaction between CGA and  $Fe^{3+}$  in hot water, showing that CGA had formed complexes with  $Fe(II)$ . From this we can infer that the compounds with  $m/z = 762.1095$ , 763.1184, 1,116.2052, and 1,117.2120 are complexes formed by CGA with  $Fe^{3+}$  and  $Fe^{2+}$  in 2:1 and 3:1 ratios, respectively.

### 3.4. Effect of CGA-metal complexes on DNA cleavage activity

#### 3.4.1. *In vitro* DNA cleavage activity

As it was still impossible to obtain pure products of CGA-metal complexes, experiments were conducted using reaction solutions of CGA and different metal ions dried under reduced pressure and dissolved in DMSO to facilitate the comparison of DNA cleavage activity among different CGA-metal complexes.

pBR322 DNA is a super-coiled double-stranded closed-loop molecule in three forms. Intact DNA usually exhibits a super-coiled conformation (SC), which has the most compact structure, and thus the fastest rate of migration in gel electrophoresis. When a nick occurs on one strand (i.e., a single-strand break), it converts to the nicked circular (NC) form, which has the slowest rate of migration in gel electrophoresis due to its loose structure. When breaks occur at the same position on both strands, it converts to the linear (L) form, and its rate of migration in gel electrophoresis is between those of SC DNA and NC DNA. Fig. S17 shows that at the doses applied in this study, 5% DMSO, the eight metal ions, CGA, as well as the reaction products of CGA with  $Ca^{2+}$ ,  $Fe^{3+}$ ,  $Mg^{2+}$ ,  $Sr^{2+}$ , and  $Zn^{2+}$  did not produce significant cleavage of pBR322 DNA after incubation for 24 h. After incubation with the reaction products of CGA and  $Cu^{2+}$ , all DNA bands disappeared,

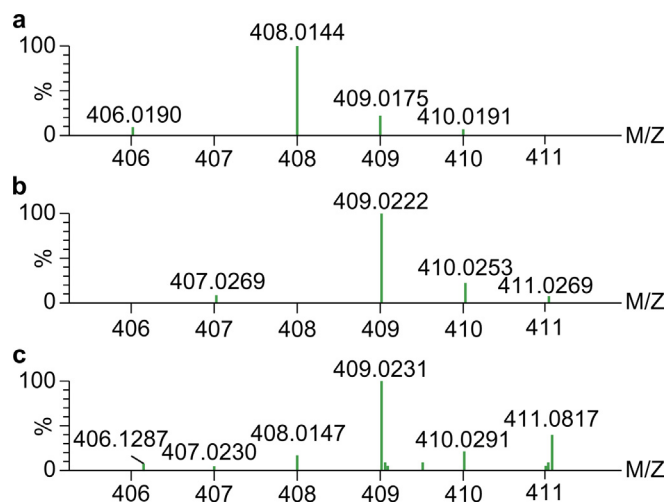


**Fig. 7** Theoretical isotopic distributions of compounds  $C_{16}H_{16}O_9Fe(III)$  (a) and  $C_{16}H_{17}O_9Fe(II)$  (b) and measured isotopic distributions (c).

indicating that the CGA-Cu complexes had a strong DNA cleavage effect. When the CGA reaction products with  $Ni^{2+}$  and  $Mn^{2+}$  were incubated with pBR322 DNA for 24 h, the SC DNA disappeared completely, and the NC DNA increased significantly, whereas a little L DNA appeared. This indicates that the CGA-Ni and CGA-Mn complexes also have a certain level of DNA cleavage activity. Based on this experiment, we explored the effect of time (Fig. S18) and concentration (Fig. S19) on the pBR322 DNA cleavage activity of the CGA and Cu(II) reaction products.

As shown in Fig. S18, when the reaction product of CGA and Cu(II) was reacted with PBR322 DNA for 0 h, a little NC DNA appeared. After incubation for 10 min, all SC DNA was cleaved into NC DNA, and a little L DNA appeared. As the incubation time increased, NC DNA gradually decreased, whereas L DNA showed an initial increase, followed by a decrease. At 2 h, most of the L DNA was cleaved into even smaller DNA fragments; therefore, no clear DNA bands could be observed on the electropherogram.

Fig. S19 shows that when the Cu(II) concentration reached 30  $\mu\text{mol/L}$  in the reaction system, all SC DNA was cleaved into NC DNA, and L DNA emerged. When the Cu(II) concentration was  $> 20 \mu\text{mol/L}$ , the NC DNA gradually decreased and virtually disappeared completely at 70  $\mu\text{mol/L}$ . In summary, these findings indicate the complexes formed by CGA and Cu(II) play a key role in DNA cleavage activity and their cleavage effect is critically related to concentration and time.

#### 3.4.2. Mechanism underlying the *in vitro* DNA cleavage activity of CGA-Cu complexes

To explore the possible mechanisms underlying the cleavage of pBR322 DNA by CGA-Cu complexes, we added EDTA and different types of free radical scavengers to the reaction system of the DNA cleavage assay. As shown in Fig. 8, when DNA was incubated with the reaction products of CGA and  $Cu^{2+}$  alone for 2 h, only a little L DNA remained. The addition of  $NaN_3$  (a singlet oxygen scavenger) did not lead to significant changes in the experimental results. The addition of the metal-ion chelating agent, EDTA, led to the disappearance of DNA cleavage activity. The addition of TEMPO (a

carbon-free radical scavenger), mannitol (a hydroxyl radical scavenger), CAT (decomposition of  $H_2O_2$ ), and SOD (superoxide anions scavenger) led to a significant increase in NC DNA and L DNA bands. CAT and SOD essentially caused the disappearance of L DNA, which implies that the DNA cleavage activity of CGA-Cu complexes was inhibited.

#### 3.5. Antibacterial activity of CGA-metal complexes

The inhibitory effects of CGA, eight metal ions, and the reaction products of CGA and the eight metal ions in hot water *S. aureus* were explored. As shown in Fig. 9, all eight metal ions had no antibacterial activity at 2.4 mmol/L. CGA showed antibacterial activity at 4.8 mmol/L, and the antibacterial effect disappeared after reacting with  $Ca^{2+}$ ,  $Mg^{2+}$ ,  $Cu^{2+}$ ,  $Fe^{3+}$ , and  $Sr^{2+}$ . The reaction products of CGA with  $Ni^{2+}$  and  $Mn^{2+}$  showed significantly stronger antibacterial effects than CGA. The reaction products of CGA and  $Mn^{2+}$  still exhibited bactericidal activity when the final CGA concentration was 1.2 mmol/L (final  $Mn^{2+}$  concentration: 0.6 mmol/L). These results indicate that the properties of metal ions have a crucial impact on the activity of the complexes.

## 4. Discussion

Current research on the formation of complexes between organic components and trace metal elements in natural medicine shows that the choice of reaction solvent significantly affects the coordination between them. For example, quercetin is an extensively studied organic compound. Quercetin and  $Cu^{2+}$  form complexes in a methanolic solution in a 1:1 ratio (Vimalraj et al., 2018). However, in an alkaline aqueous solution with a pH of 10, coordination cannot occur at 4-O and 5-OH between the two, and the complexes are formed in a quercetin/ $Cu^{2+}$  2:1 ratio. Coordination can also occur at 3'-OH and 4'-OH to form complexes at a ratio of 1:1 (Torreggiani et al., 2005). Furthermore, quercetin and  $Co^{2+}$  formed complexes in a methanolic solution in a quercetin/ $Co^{2+}$  ratio of 1:2 (Birjees Bukhari et al., 2008). However, in

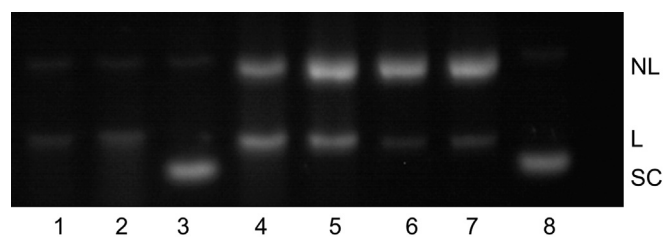


**Fig. 8** Effect of free radical inhibitors on the DNA cleavage activity of CGA and Cu(II) reaction products. Lane 1, CGA and Cu(II) reaction products; lanes 2–7, addition of  $\text{NaN}_3$ , EDTA, TEMPO, mannitol, catalase, and SOD, respectively, to the reaction system; lane 8: DNA blank control. In lanes 1–7, the final concentration of CGA was  $\mu\text{mol/L}$ , and the incubation time was 2 h.

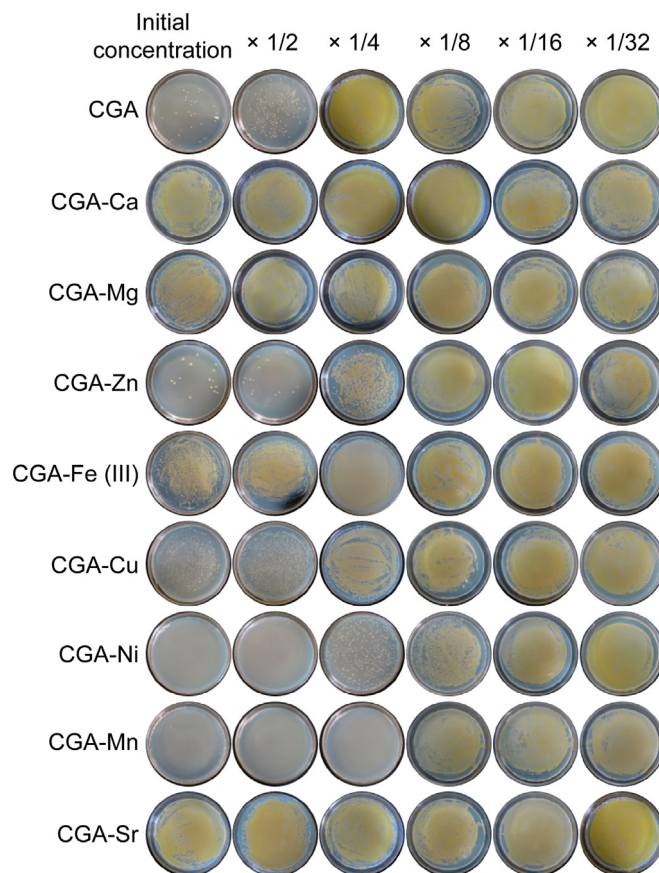


**Fig. 9** Inhibitory effects of CGA and its metal complexes on *Staphylococcus aureus*. The initial concentration of CGA was 4.8 mmol/L, and those of the metal ions were 2.4 mmol/L. All eight metal ions showed no antibacterial activity at this concentration.

ethanol, the complexes formed in a 2:1 ratio (Zhou et al., 2001). Most medicinal plants are decocted in water for consumption, whereas studies on the chemical components of medicinal plants often use methanol as an extraction solvent. Therefore, in this study, we first examined whether the aqueous and methanolic extracts of four CGA-rich medicinal plants contained metal complexes. To minimize errors during the weighing and extraction of medicinal materials, the same extract sample was divided into two aliquots, dried under reduced pressure, and dissolved in methanol and 15% FA-methanol. Our experimental findings revealed that the aqueous extract dissolved in 15% FA-methanol showed significantly higher peak areas for all chromatographic peaks. Possible reasons for this phenomenon may include the following:

- (1) Compounds with significantly higher peak areas were alkaline, and their solubility improved substantially in an acidic solution.
- (2) These compounds are aglycone components, and their corresponding glycoside components can be hydrolyzed in an acidic solution, increasing the aglycone content.
- (3) These compounds act as ligands that form complexes with metal ions during aqueous extraction, and these complexes were wholly or partially decomposed in acidic solution, increasing the content of the compounds.

Considering that aqueous extracts dissolved in methanol and 15% FA-methanol showed the same number and retention time of chromatographic peaks in the HPLC spectra, minimal changes in peak areas were observed between compounds

in methanolic extracts dissolved in methanol and 15% FA-methanol. In addition, FA is a moderately strong acid that cannot hydrolyze glycosides. The increased peak area in the HPLC spectra for aqueous extracts dissolved in 15% FA-methanol is due to the third reason. These experimental findings suggest that hot water is a suitable solvent for the formation of complexes between organic components and metal ions in medicinal plants.

Complexes of CGA with metal ions, such as  $\text{Cu}^{2+}$  (Kiss et al., 1989),  $\text{Mn}^{2+}$  (Améziame et al., 1996),  $\text{Zn}^{2+}$  (Kalinowska et al., 2020),  $\text{Fe}^{3+}$  (Mahal et al., 2005),  $\text{V}^{4+}$  (Naso et al., 2014), heavy metals ( $\text{Hg}^{2+}$ ,  $\text{Pb}^{2+}$ ,  $\text{Cu}^{2+}$ , and  $\text{Cd}^{2+}$ ) (Milić et al., 2011), and alkali metals ( $\text{Li}^+$ ,  $\text{Na}^+$ ,  $\text{K}^+$ ,  $\text{Ru}^+$ , and  $\text{Cs}^+$ ) have been previously synthesized (Kalinowska et al., 2018). Their results showed different solvents might cause CGA and metal ions to form different complexes. For example, in a buffer solution of pH 7.5, CGA could be complexed with  $\text{Cu}^{2+}$  at 1:1 and 1:2 but not with  $\text{Zn}^{2+}$  (Milić et al., 2011). In an aqueous solution, CGA could be complexed with Cu, Mn, Zn, and Fe in ratios of 1:1, 1:2, or 1:3, respectively; in a nitric acid solution, it formed complexes with Cu and Fe in a ratio of 1:1, whereas in an aqueous solution of pH > 10, it formed complexes with Zn in a ratio of 2:1 (Améziame et al., 1996). In this study, UV-Vis spectroscopy was used to confirm that CGA had complexed with the eight metal ions in hot water. ESI-TOF MS was performed to detect the CGA-metal complexes found in the reaction solution. Our results showed complexes formed by CGA and metal ions in various ratios could be found simultaneously in the reaction solution. When attempting to obtain monomers of the CGA-metal complexes through recrystallization and column chromatography, only CGA could be detected in the elution product of column chromatography (silica gel, polyamide, Sephadex LH-20, and RP-18) and not the CGA-metal complexes; this may have occurred because these metal complexes had undergone decomposition on the chromatographic media, or they were too tightly bound to the chromatographic media and therefore could not be easily eluted. The ESI-TOF MS results of recrystallized products dissolved in hot water consistently showed the simultaneous presence of CGA and its metal complexes. This may have occurred because the complexes comprising CGA and metal ions were insufficiently stable, and some may decompose into CGA and metal ions once the metal complexes are dissolved in hot water.

DNA is a crucial target for many anticancer drugs (Samsonowicz and Regulska, 2017), and the effect of metal complexes on DNA structure has been extensively researched (Ahmadi et al., 2011; Tan et al., 2009; Wang et al., 2010; Yamashita et al., 1999). Therefore, in this study, we used the double-stranded closed-loop pBR322 DNA molecule as the basis to measure the DNA cleavage activity of different CGA-metal complexes. These findings indicated EDTA could inhibit DNA cleavage; in contrast, TEMPO, mannitol, CAT, and SOD partially inhibited DNA cleavage; this implies that Cu(II) plays a significant role in DNA cleavage, while binding of CGA-Cu complexes with DNA produces carbon-free radicals, hydroxyl radicals,  $\text{H}_2\text{O}_2$ , and superoxide anions. Thus, CGA-Cu complexes can promote DNA cleavage via oxidative damage, similar to quercetin-Cu (Tan et al., 2009; Yamashita et al., 1999) and Rutin-Cu complexes (Cai et al., 2019b).

Antibiotics have been effective against bacterial infections. However, their overuse has accelerated the rate of resistance

to bacterial drugs. The rapid increase in carbapenem-resistant bacteria (carbapenems are one of the last few classes of antibiotics available) is considered a harbinger of the imminent arrival of a “public health nightmare” and “catastrophic threat.” (Mckenna, 2013). Therefore, the development of new antibiotics is an urgent requirement. The antibacterial mechanisms of metal complexes differ from those of traditional antibiotics: (1) After ligands with antibacterial activity form complexes with essential metal ions, they can enter bacteria via pathways related to the absorption, transport, and storage of essential metal ions as “Trojan horses,” killing the bacteria (Kali et al., 2016). (2) Complexes composed of non-essential metals can inhibit the absorption of essential metals in bacteria through competition, depleting essential metals in the bacteria and eventual death (Amidani et al., 2021). (3) Metal ions and ligands can enhance antibacterial activity through synergistic effects (Amidani et al., 2021; Song et al., 2009; Wanninger et al., 2015). Therefore, some researchers believe that searching for organic components or metal complexes with metal-ion binding ability in natural drugs is an effective way to discover new antibiotic candidates (Dandawate et al., 2019). Because CGA has a broad spectrum of antibacterial activity (Bajko et al., 2016; Cai et al., 2019a; Lou et al., 2011; Santana-Gálvez et al., 2017; Wang et al., 2015), we previously selected *S. aureus*, *Escherichia coli*, and *Pseudomonas aeruginosa* to examine the antibacterial activity of CGA and its various metal complexes. Our findings indicated that, at the maximum concentration used in this study, CGA and its various metal complexes only produced significant inhibitory activity against *S. aureus*.

## 5. Conclusions

Metal complexes are important active components of medicinal plants. There are limited reports on organic component-metal complexes found in medicinal plant extracts because of their wide variety, low content, lack of separation and purification methods, and easy formation only in hot water. In this study, we have established a method for discovering bioactive metal complexes rapidly and systematically from aqueous extracts of medicinal plants. Using this method, we successfully obtained chlorogenic acid-metal complexes with DNA cleavage and antibacterial activity from water extracts of medicinal plants.

## Funding

This work was supported by the Natural Science Foundation of Jiangxi Province [grant number 20212BAB206005], Science and technology research project of Education Department of Jiangxi Province [grant number GJJ211119], Open Project of Engineering Center of Jiangxi University for Fine Chemicals [grant number JFCEC-KF-2102], and Jiangxi Science and Technology Normal University Undergraduate Research Fund Project [grant number 202111318018]. The funding sources had no role in the study design, collection, analysis, or interpretation of data, in the writing of the report, or in the decision to submit the article for publication.

## CRedit authorship contribution statement

**Kangkang Zheng:** Methodology. **Yafeng Liu:** Conceptualization, Methodology. **Liang Peng:** Conceptualization, Writing – original draft. **Zhimin Li:** Writing – original draft. **Wenbin Xu:** .

## Declaration of Competing Interest

The authors declare that they have no known competing financial interests or personal relationships that could have appeared to influence the work reported in this paper.

## Acknowledgements

We would like to thank Editage (www.editage.cn) for English language editing.

## Appendix A. Supplementary material

Supplementary data to this article can be found online at <https://doi.org/10.1016/j.arabjc.2023.104835>.

## References

- Ahmadi, F., Alizadeh, A.A., Shahabadi, N., Rahimi-Nasrabadi, M., 2011. Study binding of *α*-curcumin complex to ds-DNA, monitoring by multispectroscopic and voltammetric techniques. *Spectrochim. Acta A Mol. Biomol. Spectrosc.* 79, 1466–1474. <https://doi.org/10.1016/j.saa.2011.05.002>.
- Améziiane, J., Aplincourt, M., Dupont, L., Heirman, F., Pierrard, J.-C., 1996. Thermodynamic stability of copper(II), manganese(II), zinc(II) and iron(III) complexes with chlorogenic acid. *Bull. Soc. Chim. Fr.* 133, 243–249.
- Amidani, L., Vaughan, G.B.M., Plakhova, T.V., Romanchuk, A.Y., Gerber, E., Svetogorov, R., Weiss, S., Joly, Y., Kalmykov, S.N., Kvashnina, K.O., 2021. Front cover: The application of HEXS and HERFD XANES for accurate structural characterisation of actinide nanomaterials: The case of ThO<sub>2</sub>. *Chem. Eur. J.* 27, 1–1. <https://doi.org/>.
- Bajko, E., Kalinowska, M., Borowski, P., Siergiejczyk, L., Lewandowski, W., 2016. 5-O-caffeoylquinic acid: a spectroscopic study and biological screening for antimicrobial activity. *LWT Food Sci. Technol.* 65, 471–479. <https://doi.org/10.1016/j.lwt.2015.08.024>.
- Birjees Bukhari, S., Memon, S., Mahroof Tahir, M., Bhanger, M.I., 2008. Synthesis, characterization and investigation of antioxidant activity of cobalt–quercetin complex. *J. Mol. Struct.* 892, 39–46. <https://doi.org/10.1016/j.molstruc.2008.04.050>.
- Borowska, S., Tomczyk, M., Strawa, J.W., Brzóska, M.M., 2020. Estimation of the chelating ability of an extract from *Aronia melanocarpa* L. berries and its main polyphenolic ingredients towards ions of zinc and copper. *Molecules* 25, 1507. <https://doi.org/10.3390/molecules25071507>.
- Cai, R., Miao, M., Yue, T., Zhang, Y., Cui, L., Wang, Z., Yuan, Y., 2019a. Antibacterial activity and mechanism of cinnamic acid and chlorogenic acid against *Alicyclobacillus acidoterrestris* vegetative cells in apple juice. *Int. J. Food Sci. Technol.* 54, 1697–1705. <https://doi.org/10.1111/ijfs.14051>.
- Cai, W., Zheng, K., Li, Z., Peng, L., Yin, Q., Zeng, H., Esi-Tof, M.S., 2019b. ESI-TOF MS analysis and DNA cleavage activity of rutin–metal complexes in aqueous extracts of medicinal plants. *Inorg. Chem. Front.* 6, 3184–3195. <https://doi.org/10.1039/C9QI00878K>.
- Dandawate, P., Padhye, S., Schobert, R., Biersack, B., 2019. Discovery of natural products with metal-binding properties as promising antibacterial agents. *Expert Opin. Drug Discov.* 14, 563–576. <https://doi.org/10.1080/17460441.2019.1593367>.
- Ikeda, N.E., Novak, E.M., Maria, D.A., Velosa, A.S., Pereira, R.M.N., 2015. Synthesis, characterization and biological evaluation of Rutin–zinc(II) flavonoid–metal complex. *Chem. Biol. Interact.* 239, 184–191. <https://doi.org/10.1016/j.cbi.2015.06.011>.
- Imessaoudene, A., Merzouk, H., Berroukeche, F., Mokhtari, N., Bensenane, B., Cherrak, S., Merzouk, S.A., Elhabiri, M., 2016. Beneficial effects of quercetin–iron complexes on serum and tissue lipids and redox status in obese rats. *J. Nutr. Biochem.* 29, 107–115. <https://doi.org/10.1016/j.jnutbio.2015.11.011>.
- Kali, A., Devaraj Bhuvaneshwar, P., Charles, M.V., Seetha, K.S., 2016. Antibacterial synergy of curcumin with antibiotics against biofilm producing clinical bacterial isolates. *J. Basic Clin. Pharm.* 7, 93–96. <https://doi.org/10.4103/0976-0105.183265>.
- Kalinowska, M., Bajko, E., Matejczyk, M., Kaczyński, P., Łozowicka, B., Lewandowski, W., 2018. The study of anti-/pro-oxidant, lipophilic, microbial and spectroscopic properties of new alkali metal salts of 5-O-caffeoylquinic acid. *Int. J. Mol. Sci.* 19, 463. <https://doi.org/10.3390/ijms19020463>.
- Kalinowska, M., Sienkiewicz-Gromiuk, J., Świdorski, G., Pietryczuk, A., Cudowski, A., Lewandowski, W., 2020. Zn(II) complex of plant phenolic chlorogenic acid: antioxidant, antimicrobial and structural studies. *Materials (Basel)* 13, 3745. <https://doi.org/10.3390/ma13173745>.
- Kiss, T., Nagy, G., Pécsi, M., Kozłowski, H., Micera, G., Erre, L.S., 1989. Complexes of 3, 4-dihydroxyphenyl derivatives—X. Copper (II) complexes of chlorogenic acid and related compounds. *Polyhedron* 8, 2345–2349. [https://doi.org/10.1016/S0277-5387\(00\)80295-8](https://doi.org/10.1016/S0277-5387(00)80295-8).
- Lou, Z., Wang, H., Zhu, S., Ma, C., Wang, Z., 2011. Antibacterial activity and mechanism of action of chlorogenic acid. *J. Food Sci.* 76, M398–M403. <https://doi.org/10.1111/j.1750-3841.2011.02213.x>.
- Mahal, H.S., Kapoor, S., Satpati, A.K., Mukherjee, T., 2005. Radical scavenging and catalytic activity of metal–phenolic complexes. *J. Phys. Chem. B* 109, 24197–24202. <https://doi.org/10.1021/jp0549430>.
- Mandal, B., Singha, S., Dey, S.K., Mazumdar, S., Kumar, S., Karmakar, P., Das, S., 2017. Cu<sup>II</sup> Complex of emodin with improved anticancer activity as demonstrated by its performance on HeLa and Hep G2 cells. *RSC Adv.* 7, 41403–41418. <https://doi.org/10.1039/C7RA06696A>.
- Mckenna, M., 2013. Antibiotic resistance: the last resort. *Nature* 499, 394–396. <https://doi.org/10.1038/499394a>.
- Milić, S.Z., Potkonjak, N.I., Gorjanović, S.Ž., Veljović-Jovanović, S. D., Pastor, F.T., Sužnjević, D.Ž., 2011. A polarographic study of chlorogenic acid and its interaction with some heavy metal ions. *Electroanalysis* 23, 2935–2940. <https://doi.org/10.1002/elan.201100476>.
- Naso, L.G., Valcarcel, M., Roura-Ferrer, M., Kortazar, D., Salado, C., Lezama, L., Rojo, T., González-Baró, A.C., Williams, P.A., Ferrer, E.G., 2014. Promising antioxidant and anticancer (human breast cancer) oxidovanadium (IV) complex of chlorogenic acid. synthesis, characterization and spectroscopic examination on the transport mechanism with bovine serum albumin. *J. Inorg. Biochem.* 135, 86–99. <https://doi.org/10.1016/j.jinorgbio.2014.02.013>.
- Raza, A., Xu, X., Xia, L., Xia, C., Tang, J., Ouyang, Z., 2016. Quercetin-iron complex: synthesis, characterization, antioxidant, DNA binding, DNA cleavage, and antibacterial activity studies. *J. Fluoresc.* 26, 2023–2031. <https://doi.org/10.1007/s10895-016-1896-y>.
- Raza, A., Bano, S., Xu, X., Zhang, R.X., Khalid, H., Iqbal, F.M., Xia, C., Tang, J., Ouyang, Z., 2017. Rutin–nickel complex: synthesis, characterization, antioxidant, DNA binding, and DNA cleavage activities. *Biol. Trace Elem. Res.* 178, 160–169. <https://doi.org/10.1007/s12011-016-0909-7>.
- Ruzik, L., Kwiatkowski, P., 2018. Application of CE-ICP-MS and CE-ESI-MS/MS for identification of Zn-binding ligands in goji berries extracts. *Talanta* 183, 102–107. <https://doi.org/10.1016/j.talanta.2018.02.040>.

- Samsonowicz, M., Regulska, E., 2017. Spectroscopic study of molecular structure, antioxidant activity and biological effects of metal Hydroxyflavonol complexes. *Spectrochim. Acta A Mol. Biomol. Spectrosc.* 173, 757–771. <https://doi.org/10.1016/j.saa.2016.10.031>.
- Santana-Gálvez, J., Cisneros-Zevallos, L., Jacobo-Velázquez, D.A., 2017. Chlorogenic acid: recent advances on its dual role as a food additive and a nutraceutical against metabolic syndrome. *Molecules* 22. <https://doi.org/10.3390/molecules22030358>.
- Singh, S.S., Rai, S.N., Birla, H., Zahra, W., Kumar, G., Gedda, M.R., Tiwari, N., Patnaik, R., Singh, R.K., Singh, S.P., 2018. Effect of chlorogenic acid supplementation in MPTP-intoxicated mouse. *Front. Pharmacol.* 9, 757. <https://doi.org/10.3389/fphar.2018.00757>.
- Singh, S.S., Rai, S.N., Birla, H., Zahra, W., Rathore, A.S., Dilnashin, H., Singh, R., Singh, S.P., 2020. Neuroprotective effect of chlorogenic acid on mitochondrial dysfunction-mediated apoptotic death of DA neurons in a Parkinsonian mouse model. *Oxid. Med. Cell Longev.*, 6571484 <https://doi.org/10.1155/2020/6571484>.
- Song, Y.M., Xu, J.P., Ding, L., Hou, Q., Liu, J.W., Zhu, Z.L., 2009. Syntheses, characterization and biological activities of rare earth metal complexes with curcumin and 1,10-phenanthroline-5,6-dione. *J. Inorg. Biochem.* 103, 396–400. <https://doi.org/10.1016/j.jinorgbio.2008.12.001>.
- Tan, J., Wang, B., Zhu, L.D.N.A., 2009. DNA binding and oxidative DNA damage induced by a quercetin copper(II) complex: potential mechanism of its antitumor properties. *J. Biol. Inorg. Chem.* 14, 727–739. <https://doi.org/10.1007/s00775-009-0486-8>.
- Torreggiani, A., Tamba, M., Trincherio, A., Bonora, S., 2005. Copper (II)-quercetin complexes in aqueous solutions: spectroscopic and kinetic properties. *J. Mol. Struct.* 744–747, 759–766. <https://doi.org/10.1016/j.molstruc.2004.11.081>.
- Vimalraj, S., Rajalakshmi, S., Raj Preeth, D., Vinoth Kumar, S., Deepak, T., Gopinath, V., Murugan, K., Chatterjee, S., 2018. Mixed-ligand copper(II) complex of quercetin regulate osteogenesis and angiogenesis. *Mater. Sci. Eng. C Mater. Biol. Appl.* 83, 187–194. <https://doi.org/10.1016/j.msec.2017.09.005>.
- Wang, L., Bi, C., Cai, H., Liu, B., Zhong, X., Deng, X., Wang, T., Xiang, H., Niu, X., Wang, D., 2015. The therapeutic effect of chlorogenic acid against *Staphylococcus aureus* infection through sortase A inhibition. *Front. Microbiol.* 6, 1031. <https://doi.org/10.3389/fmicb.2015.01031>.
- Wang, J.T., Xia, Q., Zheng, X.H., Chen, H.Y., Chao, H., Mao, Z.W., Ji, L.N., 2010. An effective approach to artificial nucleases using copper (II) complexes bearing nucleobases. *Dalton Trans.* 39 (8), 2128–2136. <https://doi.org/10.1039/B915392F>.
- Wang, Y., Zhang, X., Zhang, Q., Yang, Z., 2010. Oxidative damage to DNA by 1,10-phenanthroline/L-threonine copper (II) complexes with chlorogenic acid. *BioMetals* 23, 265–273. <https://doi.org/10.1007/s10534-009-9284-6>.
- Wanninger, S., Lorenz, V., Subhan, A., Edelmann, F.T., 2015. Metal complexes of curcumin—synthetic strategies, structures and medicinal applications. *Chem. Soc. Rev.* 44, 4986–5002. <https://doi.org/10.1039/C5CS00088B>.
- Wojcieszek, J., Kwiatkowski, P., Ruzik, L., 2017. Speciation analysis and bioaccessibility evaluation of trace elements in goji berries (*Lycium barbarum*, L.). *J. Chromatogr. A* 1492, 70–78. <https://doi.org/10.1016/j.chroma.2017.02.069>.
- Wojcieszek, J., Ruzik, L., 2016. Enzymatic extraction of copper complexes with phenolic compounds from açai (*Euterpe oleracea* mart.) and bilberry (*Vaccinium myrtillus* L.) fruits. *Food Anal. Methods* 9, 2105–2114. <https://doi.org/10.1007/s12161-015-0395-0>.
- Yamashita, N., Tanemura, H., Kawanishi, S., 1999. Mechanism of oxidative DNA damage induced by quercetin in the presence of Cu (II). *Mutat. Res.* 425, 107–115. [https://doi.org/10.1016/s0027-5107\(99\)00029-9](https://doi.org/10.1016/s0027-5107(99)00029-9).
- Yang, L., Tan, J., Wang, B.C., Zhu, L.C., 2014. Synthesis, characterization, and anti-cancer activity of emodin-Mn(II) metal complex. *Chin. J. Nat. Med.* 12, 937–942. [https://doi.org/10.1016/S1875-5364\(14\)60137-0](https://doi.org/10.1016/S1875-5364(14)60137-0).
- Zhou, J., Wang, L., Wang, J., Tang, N., 2001. Antioxidative and antitumour activities of solid quercetin metal (II). *Transit. Met. Chem.* 26, 57–63. <https://doi.org/10.1023/A:1007152927167>.